# DESIGN OF SILICON WIRES BASED DIRECTIONAL COUPLERS FOR MICRORING RESONATORS

**Le Trung Thanh[1], Nguyen Canh Minh, Nguyen Van Khoi[2], Bui Thi Thuy[3], Nguyen Thi Hong Loan[3]**

*[1]Vietnam National University, Hanoi (VNU); thanh.le@vnu.edu.vn*
*[2]University of Transport and Communications, Hanoi, Vietnam*
*[3]Hanoi University of Natural Resources and Environment, Hanoi, Vietnam*

**Abstract -** In this paper, we investigate the design of directional couplers and microring resonators based on silicon wires. The aim is to design the directional coupler for high performance microring resonators. The effect of microring radius, gap, silicon waveguide width on power transmission ratios is analyzed by using the 3D Eigenmode Method (EME). The behavior of microring resonators using the investigated directional coupler such as finesse (F), Q-factor and free spectral range (FSR) is investigated. The effect of the waveguide width variation on the finesse, Q-factor is also studied. The FDTD simulation shows a very good agreement with the proposed design approach.

**Key words -** integrated optics; coupled resonators; integrated optics devices; silic guidewaves; EME simulation method.

## 1. Introduction

Photonic Integrated Circuits (PIC) based on silicon on insulator (SOI) platform are very attractive in recent years. The SOI platform can provide advantages of high index contrast,creating photonic devices with compactness, CMOS compatibility and large scale production technology [1].

Microring resonators are versatile building blocks for photonic circuits especially for compact photonic structures. There are many photonic devices based on microring resonator structures such as optical filter [2], optical multiplexer [3], optical switch [4], optical delay line [5], modulator [6], differential equation solver [7], optical interleaver[8], fast and slow light [9], optical biosensor [10, 11], optical gyroscopes [12], generation of optical signals [13], etc. For accurate operation of these devices, power coupling ratios and loss of the coupler used in microring resonators are crucial and need to be carefully designed. The coupling element determines the device performance. For example, designing couplers with desired coupling power ratios is extremely important for high Q-factor and high performance for biomedical sensing based on SOImicroring resonators [10], for obtaining exact free spectral range (FSR) of dense wavelength division multiplexing and interleaver [3, 8], for high bandwidth photonic signal processing [7, 14].

Although silicon wire based directional couplers have been used in many microring resonator structures, it still lacks a detailed and accurate analysis and design for microring resonators based on the directional coupler. Silicon wire based directional couplers with two parallel waveguides has been analyzed [15, 16], but it is not suitable for applying to almost all microring resonator structures including a straight waveguide coupling with a ring waveguide. Recently, quality factor, finesse and fabrication tolerances of directional couplers used for microring resonators have been investigated [17, 18]. However, such analyses can only applied to SOI rib waveguides and microring resonators based on InGaAsP/InP.

In this paper, we present a detailed analysis and design of silicon wire based directional coupler consisting of a ring waveguide coupled with a straight waveguide used for microring resonators. The effect of silicon waveguide width, gap, and radius of the ring waveguide on the power coupling ratios is investigated. The Q-factor and finesse of microring resonators using the directional coupler is analyzed. The fabrication tolerances and wavelength sensitivity are also studied. We use the 3D EME for modeling and analysis of directional couplers and the FDTD method then is used for microring resonators to compare the results.

## 2. Modeling of the SOI directional coupler

The directional coupler based on the silicon wire used for microring resonator structures is shown in Figure1. In this work, we designed for a 1550nm center wavelength and TE polarized light. The directional coupler is made from a straight waveguide coupled with a ring waveguide with radius R. For our investigations, the height of the silicon wire is usually chosen to be $h_{co} = 220nm$ and the thick of the buried oxide (BOX) is 3µm. g is the gap of the directional coupler. The waveguide core Si ($n_{Si} = 3.45$) is covered by the SiO2 cladding ($n_{SiO_2} = 1.46$).

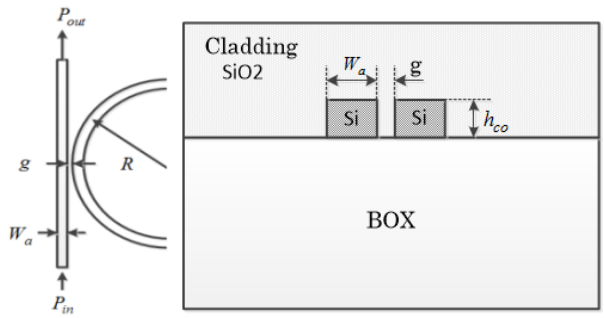


***Figure 1.*** *Schematic of the investigated SOI directional coupler for microring resonators (a) top-view and (b) cross-section view*

The directional coupler can be characterized by a transfer matrix [19, 20]

$$M = \begin{pmatrix} \tau & j\kappa \\ j\kappa & \tau \end{pmatrix} \quad (1)$$

Where $|\tau|^2 = \frac{P_{out}}{P_{in}}$ is the power transmission coefficient and $|\kappa|^2$ is the power coupling coefficient of the coupler.

Figure 2(a) and (b) show the dispersion characteristics of the silicon wire at different waveguide widths of 400, 450, 480 and 500nm, where the group index $N_g = N_{eff} - \lambda \frac{dN_{eff}}{d\lambda}$, $N_{eff}$ is the effective index calculated by the 3D EME.

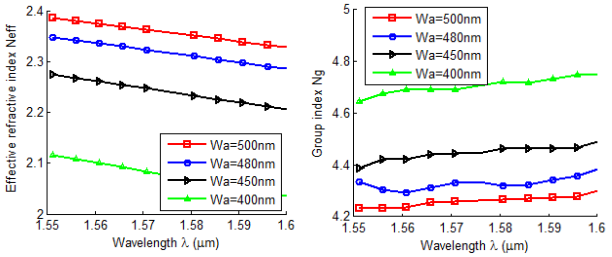


***Figure 2.*** *Effective index and group index of the silicon wire*

Transmission coefficients between straight waveguide and ring waveguide have been plotted in Figure 3 and 4 for R ranging from 5μm to 50μm and g is from 80nm to 200nm with different waveguide widths. The insets are field propagation over the coupler at $W_a = 480nm, R = 50\mu m$ and gap g=120nm and 200nm, respectively.

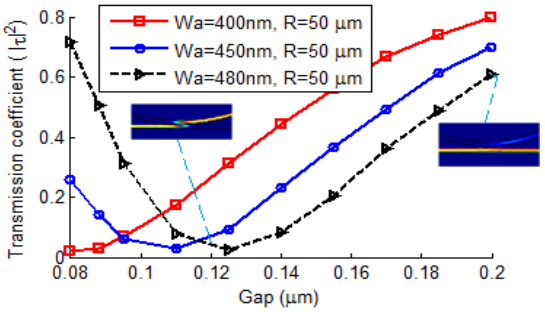


***Figure 3.*** *Power transfer between the straight and ring waveguides dependence gap and waveguide width, R=50μm*

Next we investigate the wavelength sensitivity of the coupler. The transmission coefficients are shown in Figure 5 for R=5, 20μm and gap g=87.5nm, 120nm respectively at the width Wa=400nm and wavelength ranging from 1550nm to 1600nm. The transmission coefficients decrease linearly when the wavelength increases. The decrease in transmission coefficient is proportional to the increase in radius. For R=5 μm, the coefficient $|\tau|^2$ can be expressed by $|\tau|^2 = -1.4368\lambda + 2.8362$ and $|\tau|^2 = -0.4635\lambda + 1.5627$ with R=20 μm. For a wavelength range of 25nm, the deviation of the transmission of the coupler is within 4%.

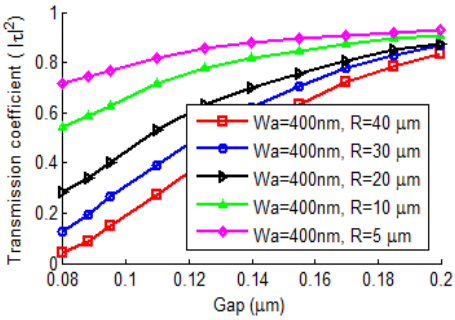


***Figure 4.*** *Power transfer between the straight and ring waveguides dependence gap and waveguide width*

## 3. Modeling of Microring resonators

Microring resonator is modelled by the transfer matrix approach as reported in [19, 21]. To further investigate the behavior of microring resonators using the coupler designed in Section 2, we examine two configurations of microring resonator structures shown in Figure 6. The microring waveguide can be coupled to one or two waveguides. Here we employ the transfer matrix approach to transfer the design parameters of the directional coupler on microring resonators.

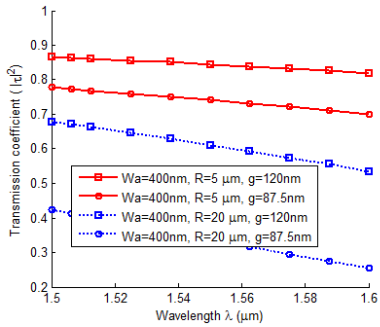


***Figure 5.*** *Wavelength dependence of the power transmission coefficient at different width and gap*

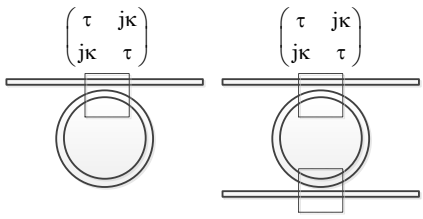


***Figure 6.*** *Two microring resonator configurations used in this study*

Based on the transfer matrix theory, the transmission of the microring resonators can be achieved. The quality factor Q of the microring resonator of Figure 6(a) and 6(b) can be derived as follows[20]:

$$Q_1 = \frac{\pi N_g L}{\lambda} \frac{\sqrt{\alpha\tau}}{1-\alpha\tau} \tag{2}$$

$$Q_2 = \frac{\pi N_g L}{\lambda} arccos\left\{\left(\frac{1+\alpha\tau^4 - 4\alpha\tau^2}{-2\alpha\tau^2}\right)\right\}^{-1} \tag{3}$$

Where $\lambda$ is the resonance wavelength of the resonators, L is the ring cavity length, $L = 2\pi R$, α is the single pass field strength attenuation which is related to the power attenuation a(1/cm) and round trip length as... For a standard silicon wire, the attenuation factor is a=2 – 3 dB/cm [22].

Another important parameter for microring resonators is the finesse F, which is defined and calculated for the single and ad-drop microring resonators by

$$F_1 = \frac{FSR}{\Delta\lambda_{FWHM}} = \pi \frac{\sqrt{\alpha\tau}}{1-\alpha\tau} \tag{4}$$

$$F_2 = \pi \frac{\tau\sqrt{\alpha}}{1-\alpha\tau^2} \tag{5}$$

Where $\Delta\lambda_{FWHM}$ is the resonance full-width-at-halft-maximum and FSR is the free spectral range. The FSR is identical for two microring resonator configurations. Figure 7 plots the FSR at different R and Wa. The FSR increases by deceasing R. We see that the FSR=2.3 nm for R=5μm, and FSR is equal to 0.25 to 2.3nm for R ranging from 5μm to 50μm. There is a slight increase in FSR when Wa decreases from 500nm to 400nm.

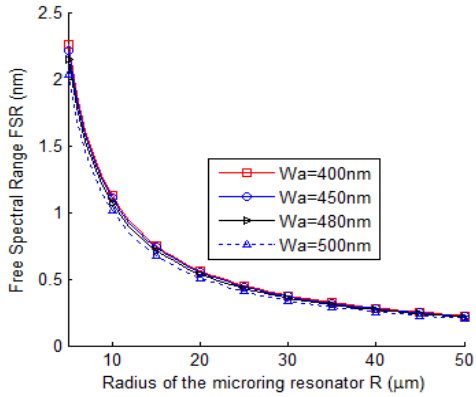


***Figure 7.*** *FSR dependence on ring radius and width of the silicon wire*

The finesses F of the single and add-drop microring resonators for gap g ranging 80nm to 200nm, R from 5 to 40μm and Wa=400nn are plotted in Figure 8(a) and (b). The finesse increases monotonically by decreasing the gap.

Figure 9 shows the Q-factor for two configurations for gap g ranging from 80nm to 200nm and Wa=400nm. We see that the Q-factor of both configurations is proportional to the radius R when the gap g>110nm. For g<110nm and R>30μm, the Finesse F and Q-factor Q are nearly independent of the radius, but for R<30 μm, the Q and F depends on the radius. For example, g=200nm, when radius increases by 5μm, the finesse F decreases by 8 while the Q-factor increases by $6x10^3$. Increasing in the gap leads to increase in Q-factor but decrease in the finesse. In addition, from the simulations of Figure 7 and 8, the finesse and Q-factor are larger for the single microring resonator than for the add-drop resonator configuration.

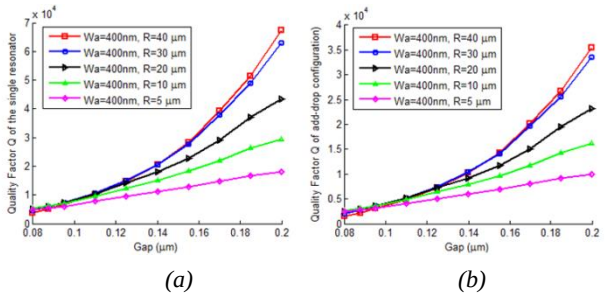


*(a)* *(b)*

***Figure 8.*** *Finesse F for single and add-drop microring resonators*

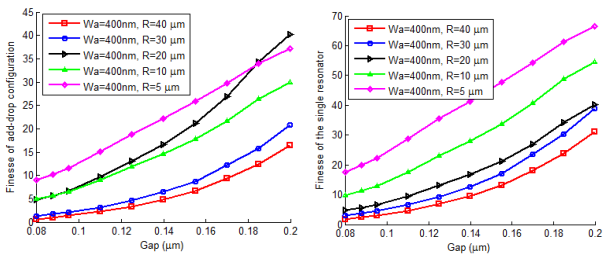


***Figure 9.*** *Q-factor for single and add-drop microring resonators*

## 4. Fabrication tolerance analysis

The simulation results for the deviation of the transmission coefficient $\Delta\tau^2$ depending on the waveguide width variation $\Delta W_a$ are shown in Figure 10. Due to the manufacturing tolerances, the variation in waveguide width occurs and leads to a new waveguide width expressed by $W = W_a \pm \Delta W_a$. Adding to the change of the transmission coefficient, the deviation of the waveguide width also leads to the change in effective index. For a positive$\Delta W_a$, the effective index is increased. For any gap and radius, a positive $\Delta W_a$ leads to a decrease in the transmission coefficient.

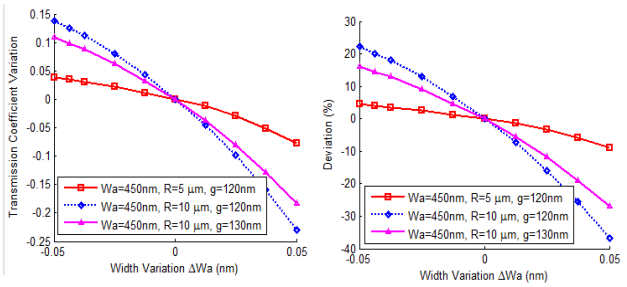


***Figure 10.*** *Change of the transmission coefficient and the deviation from the calculated value at Wa=450nm as effect of the width variation*

For $\Delta W_a = +10nm$, the transmission coefficient is decreased by 0.044 for g=120nm and 0.037 for g=130nm at the same width Wa=450nm and radius R=10μm.

While this coefficient is decreased only by 0.012 if the ring radius R=5μm. As a result, the transmission coefficient of the coupler is quite stable for a smaller ring radius and larger gap. For a width variation within ±20nm, a deviation of the transmission coefficient of 13% can be obtained.

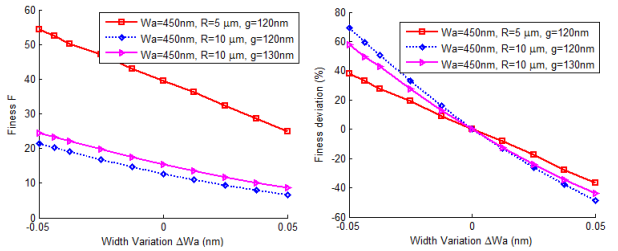


*(a)* *(b)*

***Figure 11.*** *Calculated effects of the deviation of waveguide widths on the behavior of the microring resonator (a) change in the finess F and (b) finesse deviation from the normalized value*

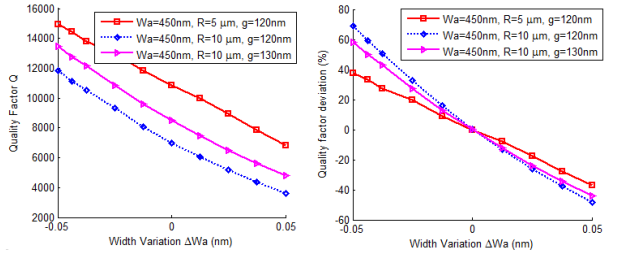


*(a)* *(b)*

***Figure 12.*** *Calculated effects of the deviation of waveguide widths on the behavior of the microring resonator (a) change in the Q-factor and (b) Q-factor deviation from the normalized value*

The calculated results for the change of the finesse F and Q-factor as well as the relative deviation from the normalized values in % are presented in Figure 11 and 12. The graphs are plotted over the waveguide width variation $\Delta W_a$ for different radius and gap. For a positive $\Delta W_a$, both finesse and Q-factor increase. For a waveguide width variation of ±10nm, the maximal finesse change of 16%

and Q-factor change of 27% is achieved.

## 5. FDTD Simulation

To verify the accuracy of the transfer matrix analysis, we compare the results obtained with the FDTD. For our FDTD simulations, the radius of the microring resonator is to be $R = 5\mu m$, the waveguide width is $W_a = 400nm$, the gap between the microring waveguide and the straight waveguide is chosen to be g=160nm in order for the power transmission coupling to be $|\tau|^2 = 0.9$.

In our FDTD simulation, we take into account the wavelength dispersion of the silicon waveguide as shown in Figure 2. We employ the design of the directional coupler presented in the previous section as the input for the FDTD. A Gaussian light pulse of 15fs pulse width is launched from the input to investigate the transmission characteristics of the device. The grid size $\Delta x = \Delta y = 0.02$nm and $\Delta z = 0.02nm$ are chosen in our simulations. The simulation results for field propagation over the single microring resonator based on the designed directional coupler are shown in Figure 13. We see that the FDTD simulation has a very good agreement with the proposed analysis.

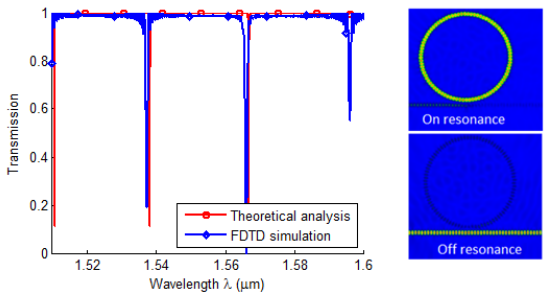


***Figure 13.*** *FDTD simulation of the single microring resonator compared with the transfer matrix approach integrated with the proposed analysis*

## 6. Conclusion

We have presented a detailed analysis and design of the directional coupler based on silicon wires. We have focused on the behavior of the directional coupler used for microring resonator structures. The parameters of the directional coupler are taken into consideration in order to achieve the desired design characteristics. The transmission coefficient of the coupler, finesse, Q-factor of the investigated directional coupler based microring resonators have been investigated. In addition, the sensitivity of the coupler to variations of the waveguide width, gap and wavelength is also presented. Our method approach can be applied and extended to the design of microring resonator structures using directional couplers based on the silicon wires.

**Acknowledgements**

This research is funded by Vietnam National Foundation for Science and Technology Development (NAFOSTED) under grant number "103.02-2013.72" and Vietnam National University, Hanoi (VNU) under project number QG.15.30.

## REFERENCES

[1] M. Jamal Deen and Prasanta Kumar Basu, *Silicon Photonics: Fundamentals and Devices*: Wiley Series in Materials for Electronic & Optoelectronic Applications, 2012.

[2] C. Vázquez, S. Vargas, J. M. S. Pena *et al.*, "Tunable optical filters using compound ring resonators for DWDM", *IEEE Photonics Technology Letters*, vol. 15, pp. 1085-1087, 2003.

[3] D. T. H. Tan, A. Grieco, and Y. Fainman, "Towards 100 channel dense wavelength division multiplexing with 100GHz spacing on silicon", *Optics Express*, vol. 22, pp. 10408-10415, 2014.

[4] Sang-Yeon Cho and Richard Soref, "Interferometric microring-resonant 2×2 optical switches", *Optics Express*, vol. 16, pp. 13304-13314, 2008.

[5] F. Liu, Q. Li, and Z. Zhang et al., "Optically tunable delay line in silicon microring resonator based on thermal nonlinear effect", *IEEE Journal of Selected Topics in Quantum Electronics*, vol. 14, pp. 706 - 712, 2008.

[6] Yingtao Hu, Xi Xiao, Hao Xu *et al.*, "High-speed silicon modulator based on cascaded microring resonators", *Optics Express*, vol. 20, pp. 15079-15085, 2012.

[7] Ting Yang, Jianji Dong, Liangjun Lu *et al.*, "All-optical differential equation solver with constant-coefficient tunable based on a single microring resonator", *Scientific Reports*, vol. 4, July 2014.

[8] J. Song, H. Zhao, and Q. Fang et al., "Effective thermo-optical enhanced cross-ring resonator MZI interleavers on SOI", *Optics Express*, vol. 16, pp. 21476-21482, 2008.

[9] Chris Fietz and Gennady Shvets, "Simultaneous fast and slow light in microring resonators", *Optics Letters*, vol. 32, pp. 3480-3482, 2007.

[10] C. Ciminelli, F. Dell'Olio, D. Conteduca *et al.*, "High performance SOI microring resonator for biochemical sensing", *Optics & Laser Technology*, vol. 59, pp. 60-67, 2014.

[11] G Testa, G Persichetti, and R Bernini, "Optimization of a Hybrid Silicon-Polymer Optical Ring Resonator", *Sensors, Springer*, vol. 319, pp. 259-263, 2015.

[12] Mario N. Armenise, Caterina Ciminelli, Francesco Dell'Olio *et al.*, *Advances in Gyroscope Technologies*: Springer, 2011.

[13] IS Amiri, A Shahidinejad, and J Ali, "Generating of 57–61 GHz frequency band using a panda ring resonator", *Quantum Matter*, 2014.

[14] Fangfei Liu, Tao Wang, Li Qiang *et al.*, "Compact optical temporal differentiator based on silicon microring resonator", *Optics Express*, vol. 16, pp. 15880-15886, 2008.

[15] Yu-jun Quan, Pei-de Han, Qi-jiang Ran *et al.*, "A photonic wire-based directional coupler based on SOI", *Optics Communications*, vol. 281, pp. 3105–3110, 2008.

[16] Vittorio M.N Passaro, Francesco Dell'Olio, Branislav Timotijevic *et al.*, "Polarization-insensitive directional couplers based on SOI wire waveguides", *The Open Optics Journal*, vol. 2, pp. 6-9, 2007.

[17] C. Ciminelli, V. M.N. Passaro, F. Dell'Olio *et al.*, "Quality factor and finesse optimization in buried InGaAsP/InP ring resonators", *The Journal of European Optical Society*, vol. 4, pp. 09032-, 2009.

[18] Andreas Prinzen, Michael Waldow, and Heinrich Kurz, "Fabrication tolerances of soi based directional couplers and ring resonators", *Optics Express*, vol. 21, pp. 17212-17220, 2013.

[19] A. Yariv, "Universal relations for coupling of optical power between microresonators and dielectric waveguides", *Electronics Letters*, vol. 36, pp. 321–322, 2000.

[20] Ioannis Chremmos, Otto Schwelb, and Nikolaos Uzunoglu (Editors), *Photonic Microresonator Research and Applications*: Springer, 2010.

[21] D.G. Rabus, *Integrated Ring Resonators – The Compendium*: Springer-Verlag, 2007.

[22] Yurii Vlasov and Sharee McNab, "Losses in single-mode silicon-on-insulator strip waveguides and bends", *Optics Express*, vol. 12, pp. 1622-1631, 2004.

*(The Board of Editors received the paper on 05/03/2015, its review was completed on 06/26/2015)*